Journal of ELECTRONIC MATERIALS, Vol. 29, No. 10, 2000

Phase Equilibria and the Related Properties of Sn-Ag-Cu Based Pb-free Solder Alloys

I. OHNUMA,[1] M. MIYASHITA,[1] K. ANZAI,[2] X.J. LIU,[1]
H. OHTANI,[3] R. KAINUMA,[1] and K. ISHIDA [1]

1.—Tohoku University, Department of Materials Science, Graduate School of Engineering, Aoba-yama 02, Sendai 980-8579, Japan. 2.—Tohoku University, Department of Materials Processing, Graduate School of Engineering, Aoba-yama 02, Sendai 980-8579, Japan. 3.—Tohoku University, Center for Interdisciplinary Research, Aoba-yama, Sendai 980-8578, Japan

We have recently developed a thermodynamic database for micro-soldering alloys which consists of the elements Pb, Bi, Sn, Sb, Cu, Ag, Zn, and In. In this paper, the phase equilibria and the related thermodynamic properties of the Sn-Ag-Cu base alloys are presented using this database, alloy systems being one of the promising candidates for Pb-free solders. The isothermal section diagrams of the Sn-Ag-Cu ternary system were experimentally determined by SEM-EDS, x-ray diffraction and metallographic techniques. Based on the present results as well as the previous data on phase boundaries and thermochemical properties, thermodynamic assessment of this system was carried out. The isothermal and vertical section diagrams, liquidus surface, mass fractions of the phase constitution, etc., were calculated. The predictions of surface energy and viscosity were also investigated. Moreover, a non-equilibrium solidification process using the Scheil model was simulated and compared with the equilibrium solidification behavior in some Sn-Ag-Cu base alloys. Calculated results based on the Scheil model were incorporated into a three-dimensional solidification simulation and the prediction of practical solidification procedures was performed.

Key words: Phase diagrams, thermodynamics database, Pb-free solders, computer simulation, Sn-Ag-Cu based alloys, solidification

INTRODUCTION

Lead-tin base solders have long been the most popular materials for electronic packaging because of their low cost and superior properties required for interconnecting electronic components. However, the toxic nature of lead and the increasing awareness of its adverse effect on environment and health have given rise to the pressing need for development of lead-free solders in recent years. Nontoxic substitute materials should satisfy the following criteria if they are to serve as effective replacements for lead. They should (1) be in plentiful supply, (2) be characterized by melting and solidifying temperatures not too different from the existing solder alloys, (3) be highly conductive, (4) possess strength and toughness, (5) be wettable, and (6) cost the same as lead-bearing solder. It has been suggested earlier that the Sn-Ag-Cu system could satisfy the foregoing criteria as a promising candidate for lead-free solders;[1] however, its high melting temperature prevents it from being applied to the practical soldering process. Thus, further consideration should be given to alloy design in the effort to develop lead-free solders. Recently, the author's group[2,3] has developed a thermodynamic database for use in designing micro-soldering alloys containing the elements Pb, Bi, Sn, Sb, Cu, Ag, Zn, and In based on the CALPHAD method,[4] which is strongly expected to support an efficient alloy design. In this paper, the phase equilibria and the related properties of the Sn-Ag-Cu system calculated using this database are presented. In addition, three-dimensional simulation of the solidification process making use of calculated properties is demonstrated.

(Received March 13, 2000; accepted April 25, 2000)

EXPERIMENTAL PROCEDURE

Sn-Ag-Cu ternary alloys were made by melting pure Ag (99.99 mass%), Sn (99.999 mass%), and Cu (99.99 mass%) in evacuated transparent quartz capsules at 1150°C for 2 h. After annealing at 300°C,

Table I. Nominal Composition and Phase Equilibria in the Sn-Ag-Cu Alloys

Equilibria phase1 / phase2 / phase3	mass%Ag / mass%Cu (nominal)	Annealing temperature /°C	mass%Ag / mass%Cu (measured) phase1	phase2	phase3
ε-Ag_3Sn / η-Cu_6Sn_5 / L	20.0 / 20.0	300	70.6 / 1.1	1.2 / 39.1	1.4 / 3.8
ε-Ag_3Sn / η-Cu_6Sn_5 / ε-Cu_3Sn	20.0 / 40.0	300	69.3 / 3.0	1.4 / 39.4	1.8 / 60.0
(Ag) / (Cu) / δ-$Cu_{41}Sn_{11}$	20.0 / 60.0	300	79.9 / 12.9	4.6 / 85.1	7.5 / 65.8
ε-Ag_3Sn / ε-Cu_3Sn / L	30.0 / 15.0	400	69.2 / 2.4	2.4 / 59.9	30.0 / 8.4
(Ag) / ε-Cu_3Sn / δ-$Cu_{41}Sn_{11}$	35.0 / 40.0	400	87.7 / 6.2	— / —	6.2 / 62.1
(Ag) / (Cu) / δ-$Cu_{41}Sn_{11}$	40.0 / 40.0	400	90.2 / 4.7	3.1 / 83.2	4.8 / 63.7
ζ-Ag / ε-Cu_3Sn / L	48.0 / 20.0	500	73.7 / 3.5	4.3 / 58.6	52.1 / 15.7
ζ-Ag / ε-Cu_3Sn / —	39.5 / 33.0	500	80.5 / 4.5	3.9 / 58.9	—
(Ag) / (Cu) / δ-$Cu_{41}Sn_{11}$	20.0 / 60.0	500	89.8 / 4.5	4.2 / 80.7	8.2 / 67.9

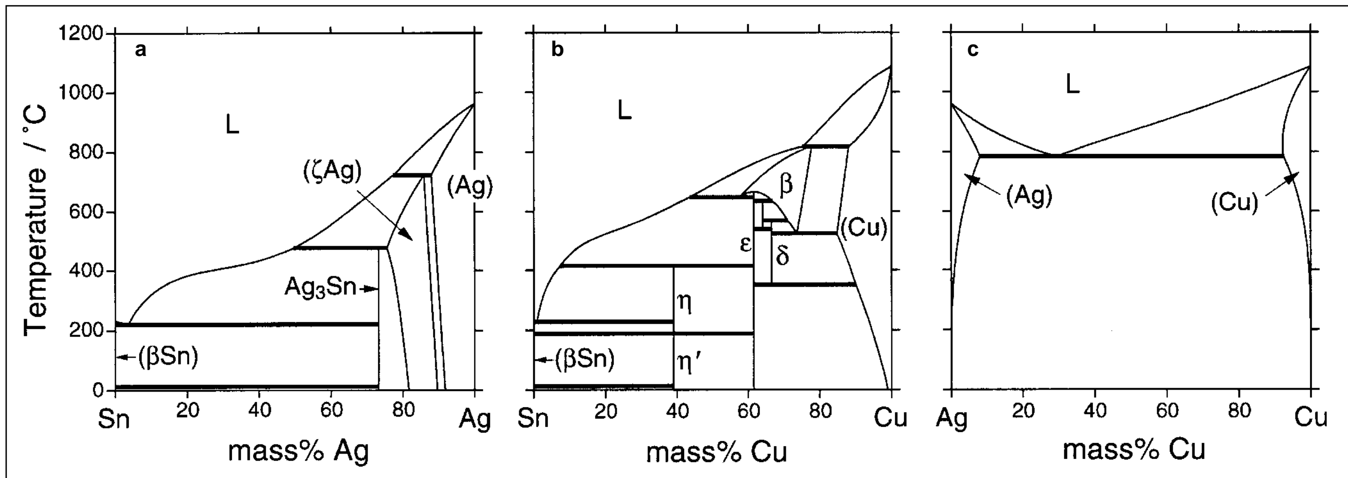

Fig. 1. Calculated phase diagrams of (a) Sn-Ag, (b) Sn-Cu, and (c) Ag-Cu binary systems.

400°C and 500°C and quenching into iced water, microstructural examination of each specimen was carried out by optical microscopy using an etchant solution made up of methyl-alcohol and a slight amount of hydrochloric acid solution. Equilibrium compositions in multi-phase specimens were determined by energy dispersive x-ray spectroscopy (SEM-EDS) using a standard calibration method. Crystal structures were identified by x-ray diffraction. The results of analysis are shown in Table I.

THERMODYNAMIC EVALUATION

The thermodynamic assessment of the Sn-Ag-Cu ternary system is based on the following binary systems: Ag-Sn,[5] Ag-Cu, [6] and Cu-Sn [7] and calculated phase diagrams of each binary system are shown in Fig. 1. In these assessments, most of the lattice stabilities of pure elements were taken from the SGTE (Scientific Group Thermodata Europe) database compiled by Dinsdale.[8] Otherwise, there are two suggestions on the lattice stability of the metastable hcp-Sn phase. One was proposed by Kattner et al.[5] where the metastable melting temperature of hcp-Sn, T_m^{hcp-Sn}, is assumed to be 226°C, and the other was suggested by Karakaya and Thompson,[9] T_m^{hcp-Sn} = 155°C. Tonkov[10] measured melting temperatures of the hcp-Sn phase

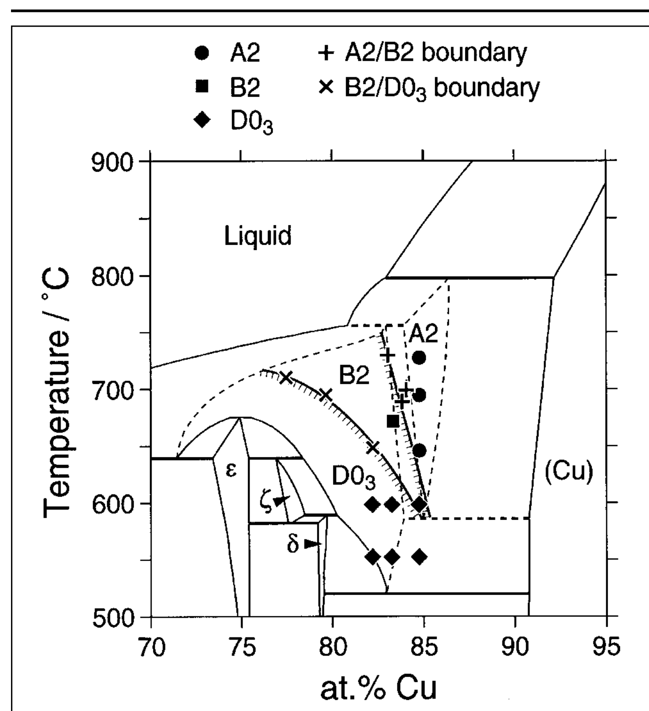

Fig. 2. A2/B2/D0$_3$ boundaries in the bcc phase of the Sn-Cu binary system.

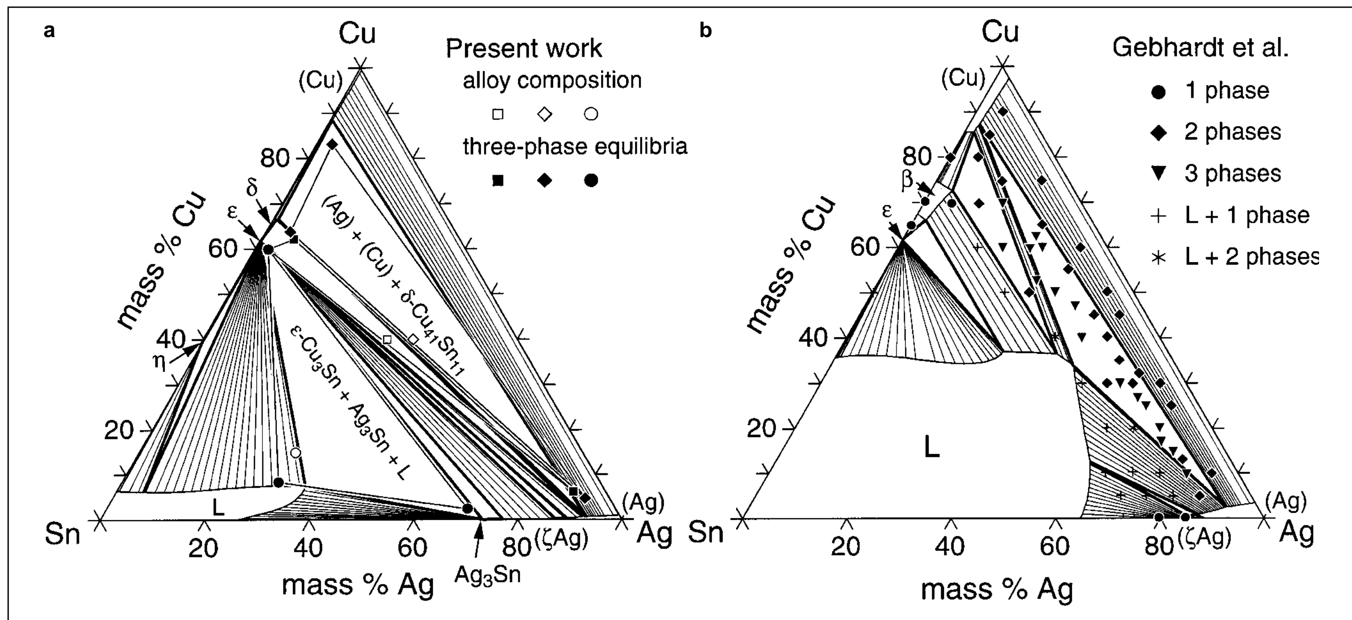

Fig. 3. Isothermal section diagrams of the Sn-Ag-Cu ternary system at (a) 400°C and (b) 600°C.

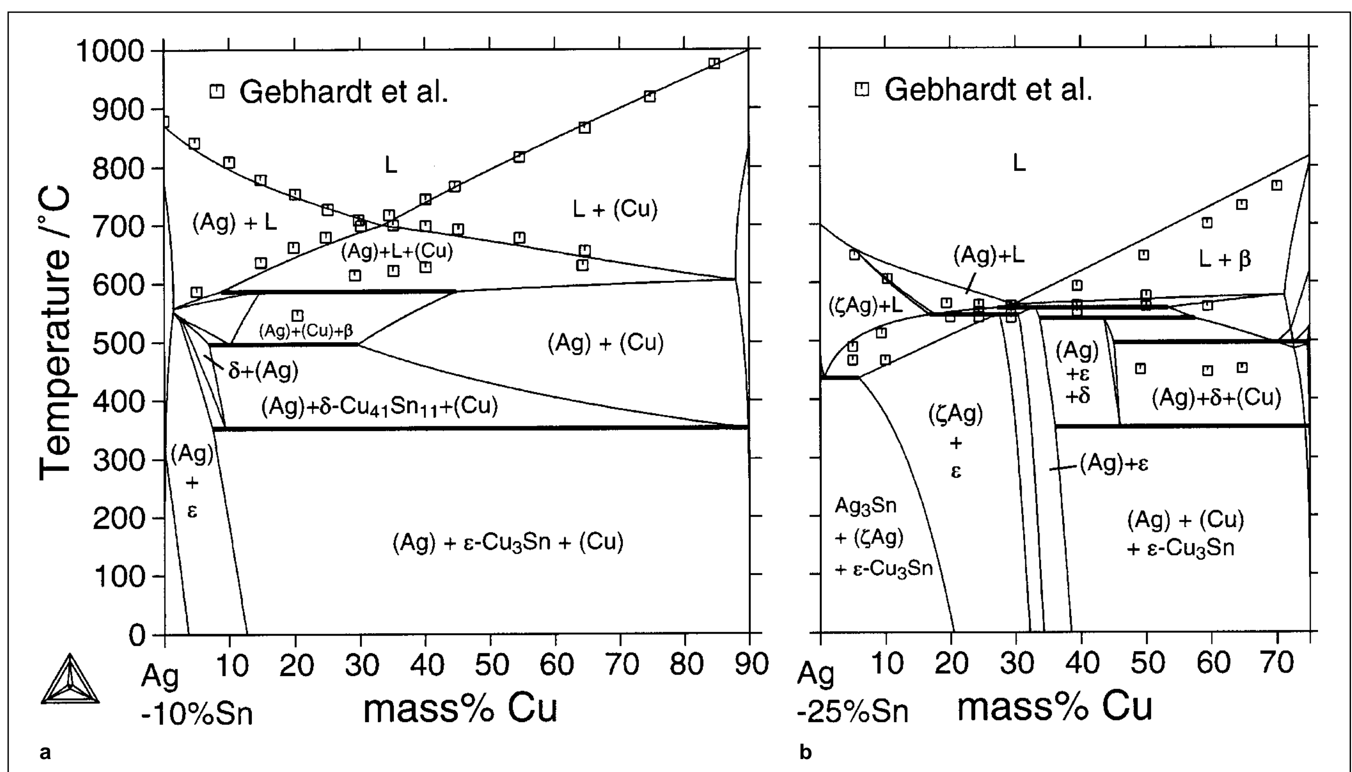

Fig. 4. Vertical section diagrams of (a) 10 mass%Sn-Ag-Cu and (b) 25 mass%Sn-Ag-Cu alloys.

under high pressure conditions and determined the metastable value extrapolated to the atmospheric pressure to be 160°C. In accordance with this result, Karakaya's lattice stability was accepted as previously reported[11] and the interaction parameter of the hcp phase, (ζAg), in the Ag-Sn binary system was evaluated by our group.[12] Other lattice stabilities of metastable phases and interaction parameters of metastable hcp and bcc phases in the Ag-Cu system were evaluated in the present study. In the Cu-Sn binary system, the two-phase separation between the disordered bcc phase, β (A2), and the ordered one, γ($D0_3$), was proposed to appear[13,14] as shown by dashed curves in Fig. 2. However, recent experimental results[15] shown by marks and hatched curves superimposed on Fig. 2 suggest that the boundaries are the second order reaction between A2, B2, and $D0_3$ phases instead of the first order two-phase separation. Strictly

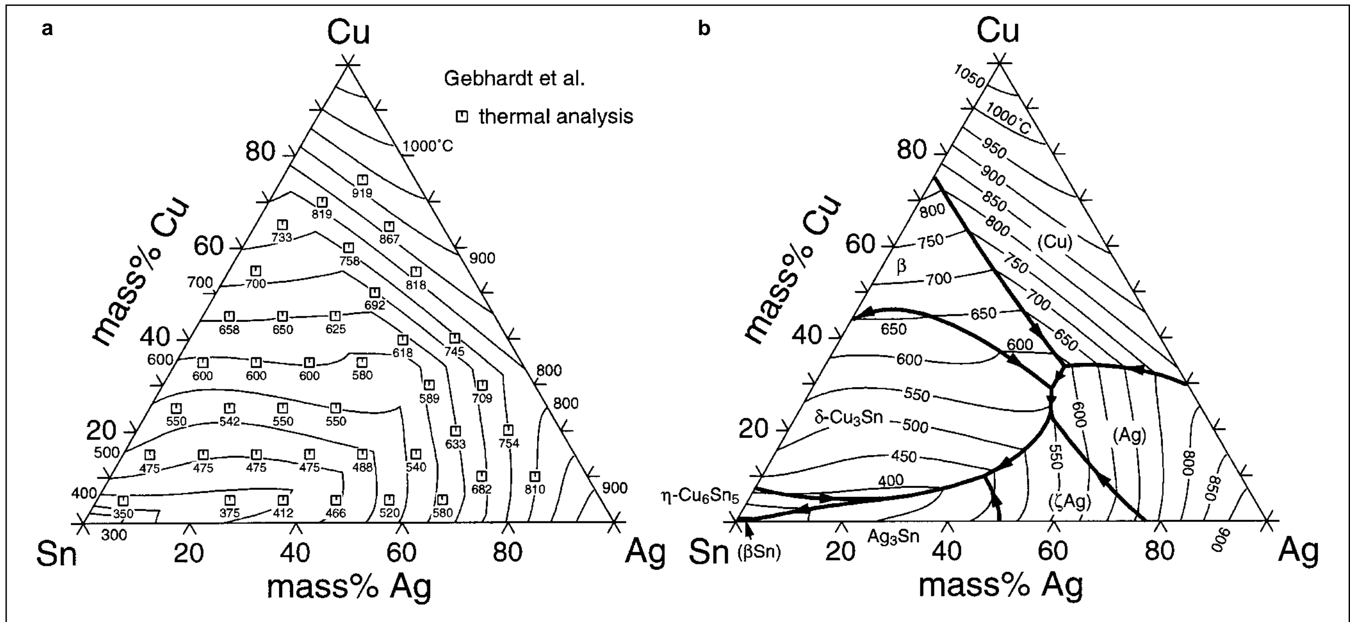

Fig. 5. (a) Comparison of calculated and experimental data on liquidus surface and (b) projection of liquidus surface.

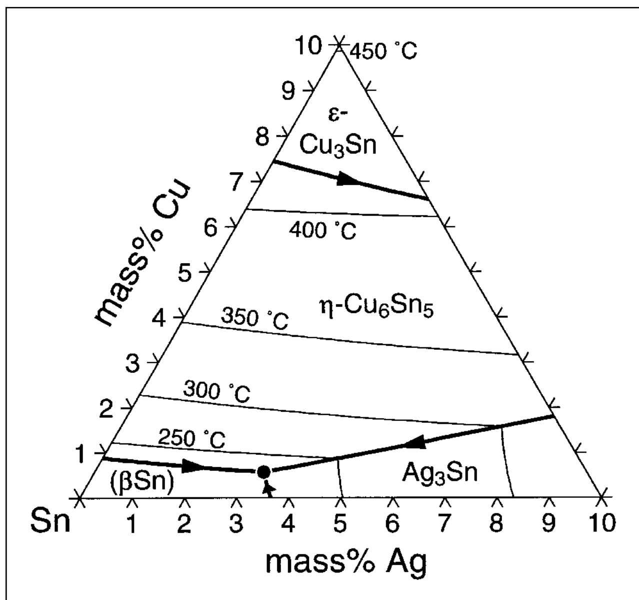

Fig. 6. Projection of liquidus surface in Sn-rich portion.

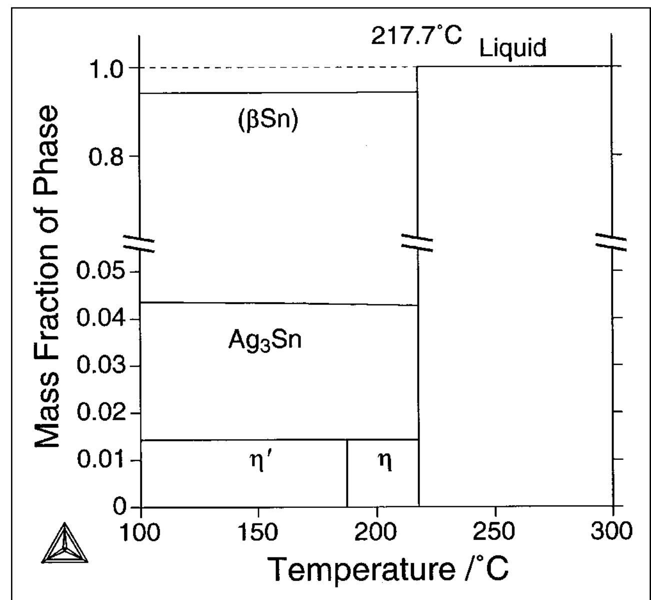

Fig. 7. Mass fraction of phases vs. temperature of Sn-Ag-Cu ternary eutectic alloy.

speaking, a four-sublattice description is needed to describe these A2/B2/D0$_3$ ordering reactions. This kind of thermodynamic treatment is, however, rather complicated and is inadequate for extending the database to multicomponent systems. Hence, these three bcc phases are taken to be one homogeneous phase whose Gibbs energy is described by the sub-regular solution approximation; its interaction parameters were newly evaluated in the present assessment. Finally, thermodynamic parameters were arranged within the framework of the Thermo-Calc software.[16]

EXPERIMENTAL AND CALCULATION RESULTS

Figures 3 and 4 show the calculated isothermal section diagrams at 400°C and 600°C and vertical section diagrams at 10 mass% and 20 mass% Sn, respectively, superimposed with the present experimental results and the experimental data of Gebhaldt et al.[17] As shown in these diagrams, the agreement between experimental data and calculations is quite satisfactory. Figure 5a shows a comparison between the calculated liquidus surface and the experimental data by Gebhaldt et al.;[17] reaction paths are superimposed in Fig. 5b. Concerning the substitute material for the Pb-Sn eutectic solder alloy whose melting temperature is 183°C, one should pay attention to Sn-rich corner of the liquidus surface diagram. Figure 6 shows the partial liquidus surface projection focused

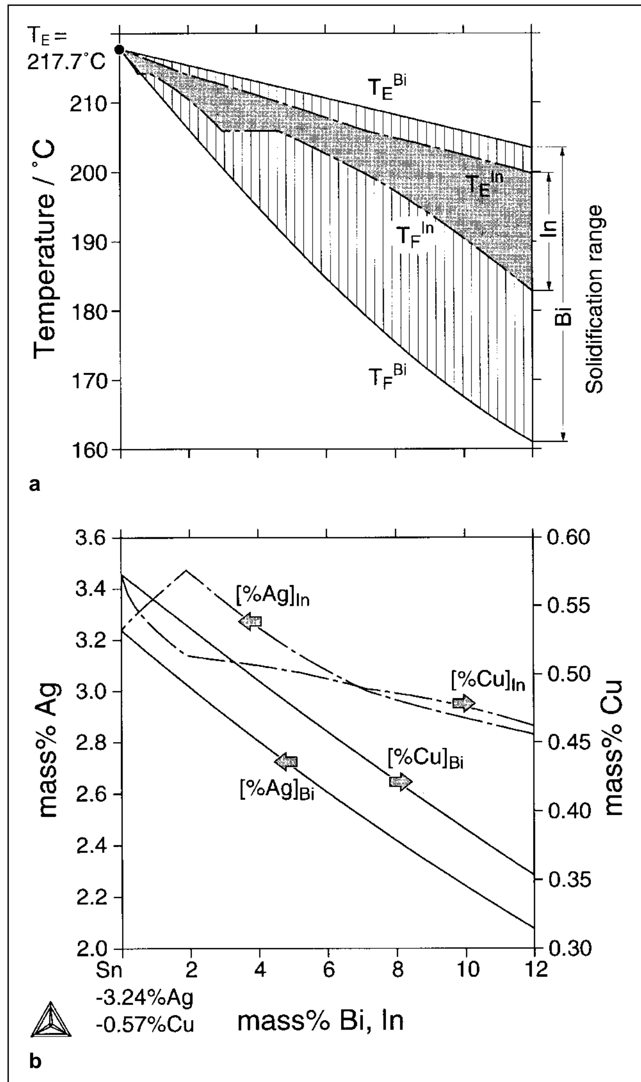

Fig. 8. Effect of Bi and In on the Sn-Ag-Cu ternary eutectic reaction.

on the following ternary eutectic reaction at 3.24 mass% Ag, 0.57 mass% Cu, and 217.7°C:

$$L \rightarrow (\beta\ Sn) + \eta - Cu_6Sn_5 + Ag_3Sn \qquad (1)$$

Figure 7 shows the phase fraction change of the ternary eutectic alloy during solidification. The melting temperature is the most significant property of substitute material for the Pb-bearing solder alloys now in use; however, the melting temperature of the ternary eutectic alloy (217.7°C) in the Sn-Ag-Cu system is much higher than that of the Pb-Sn eutectic solder (183°C). For depressing the melting temperature, the effect of additional elements, such as Bi and In, should be taken into account. Figure 8a shows that the effect of Bi and In on the ternary eutectic reaction described by Eq. 1. Calculation was made along the locus of following reaction:

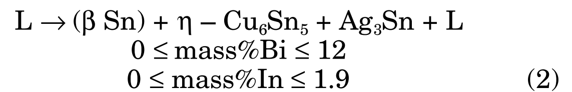

$$L \rightarrow (\beta\ Sn) + \eta - Cu_6Sn_5 + Ag_3Sn + L \\ 0 \le \text{mass\%Bi} \le 12 \\ 0 \le \text{mass\%In} \le 1.9 \qquad (2)$$

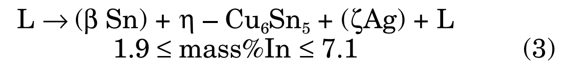

$$L \rightarrow (\beta\ Sn) + \eta - Cu_6Sn_5 + (\zeta Ag) + L \\ 1.9 \le \text{mass\%In} \le 7.1 \qquad (3)$$

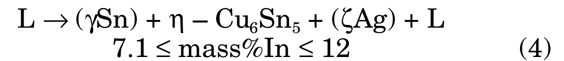

$$L \rightarrow (\gamma Sn) + \eta - Cu_6Sn_5 + (\zeta Ag) + L \\ 7.1 \le \text{mass\%In} \le 12 \qquad (4)$$

The temperature of the reaction falls and solidification range increases with increasing Bi and In content. The contents of Ag and Cu in the eutectic melt also change depending on the content of these additional elements and could be calculated as shown by Fig. 8b. This indicates that the relationship between the melting temperature and composition of the alloy should be maintained for efficient alloy design.

Thermodynamic description based on the CALPHAD method provide other properties as well as phase diagrams and contribute to alloy design of

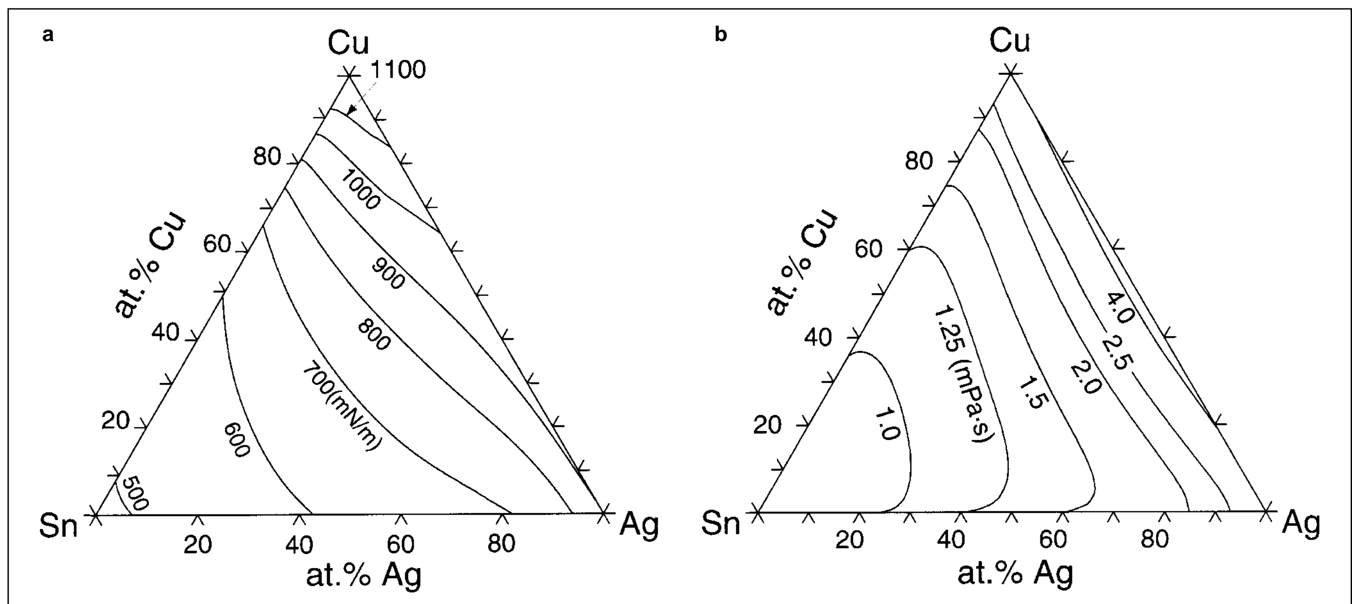

Fig. 9. Calculated (a) surface energy and (b) viscosity of Sn-Ag-Cu alloys at 1000°C.

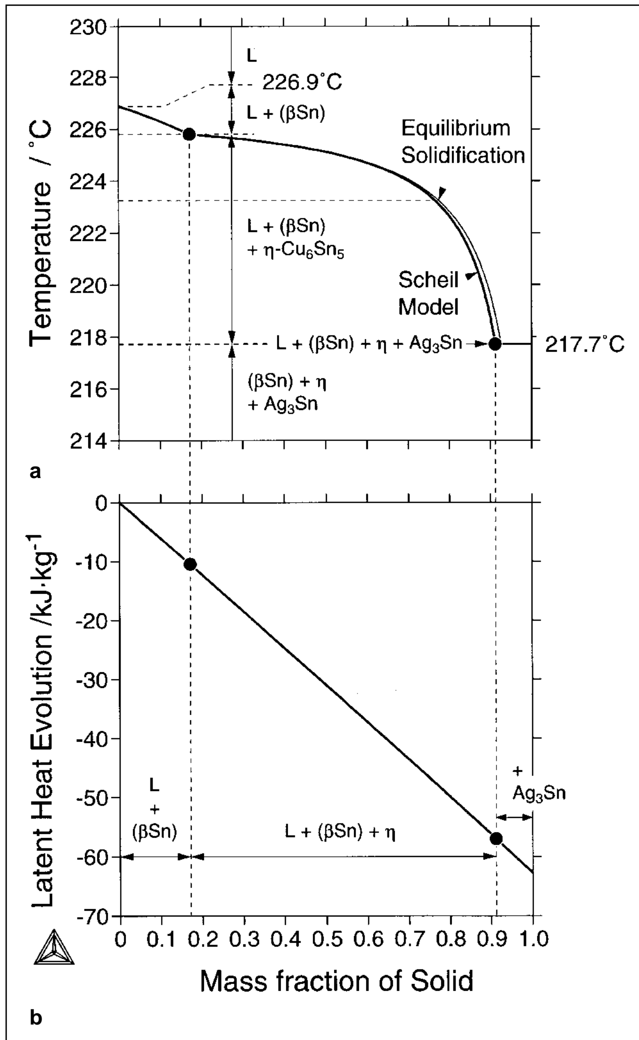

Fig. 10. (a) Mass fraction of solid phases vs. temperature and (b) latent heat evolution during solidification of Sn-0.3%Ag-0.7%Cu alloy, where thin and thick solid lines represent equilibrium solidification and non-equilibrium solidification by the Scheil model, respectively.

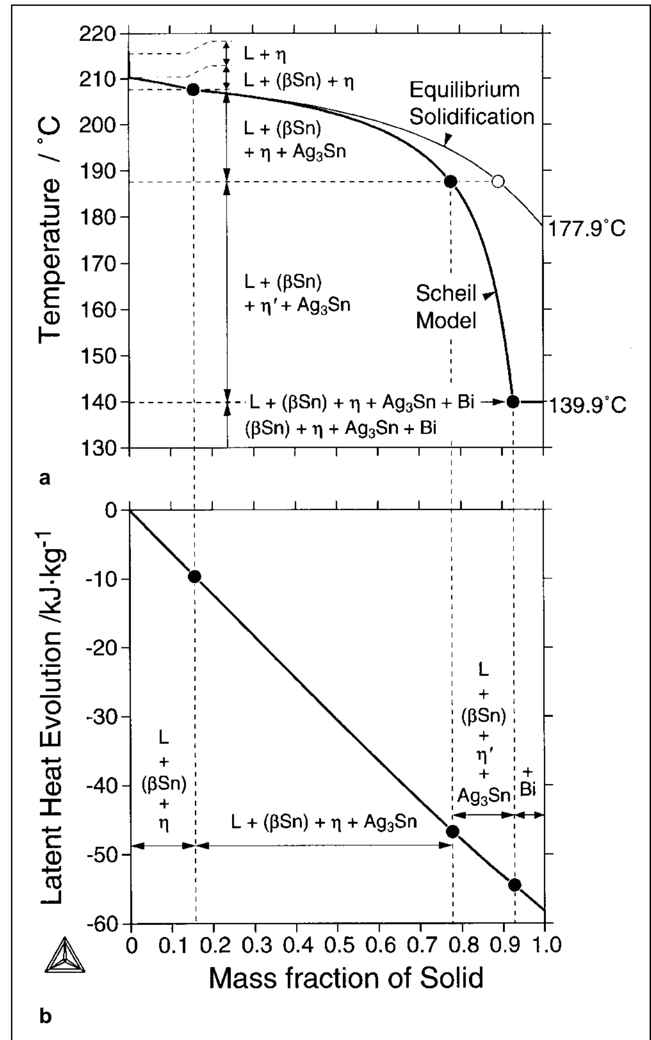

Fig. 11. (a) Mass fraction of solid phases vs. temperature and (b) latent heat evolution during solidification of Sn-2.0%Ag-0.5%Cu-7.5%Bi alloy, where thin and thick solid lines represent equilibrium solidification and non-equilibrium solidification by the Scheil model, respectively.

the micro-soldering alloys. One example is a property of melt such as the surface tension and viscosity shown in Fig. 9, which can be calculated using the thermodynamic models proposed by Butler[18] and Tanaka,[19] and Seetharaman and Sichen,[20] respectively. Such information is expected to be helpful in assessing the melting behavior and the feasibility of Pb-free solder manufacture.

In the practical solidification process, non-equilibrium rather than equilibrium solidification is often observed and could be easily simulated by the Scheil module of Thermo-Calc. In addition, calculated data such as the mass fraction of solid phases, latent heat evolution, composition of growing solid phases, etc., can be employed for predicting the three-dimensional solidification process by ADSTEFAN (advanced solidification technology for foundry aided by numerical simulation), which was developed by Niyama and Anzai.[21]

Three kinds of Sn-Ag-Cu based alloys, Sn-3.24%Ag-0.57%Cu (ternary eutectic alloy), Sn-0.3Ag-0.7Cu, and Sn-2.0Ag-0.5Cu-7.5Bi [22] (mass%) were chosen for solidification simulation, all of them being promising candidates as alternatives to Pb-Sn solders. Figure 10a shows the calculated mass fraction of the solid phases vs. the temperature variation of Sn-0.3Ag-0.7Cu alloy under equilibrium and Scheil-model solidification conditions. In both cases, the solidification starts at 226.9°C with the primary crystals of (βSn) and is terminated when it reaches the ternary eutectic reaction at 217.7°C. The difference between the two cases seems to be quite small. The latent heat evolution during the solidification process due to the Scheil model is shown in Fig. 10b. The solidification of Sn-2.0Ag-0.5Cu-7.5Bi alloy, so-called alloy-H, was also simulated and the result is shown in Fig. 11a. The solidification starts with the primary crystals of η-Cu_6Sn_5; it proceeds substantially, however, with the growth of (βSn) at the beginning. After commencement of the crystallization of Ag_3Sn phase, the liquid phase would disappear at 177.9°C under the equilibrium solidification condition. According to the Scheil model, Bi is concentrated in the liquid phase during

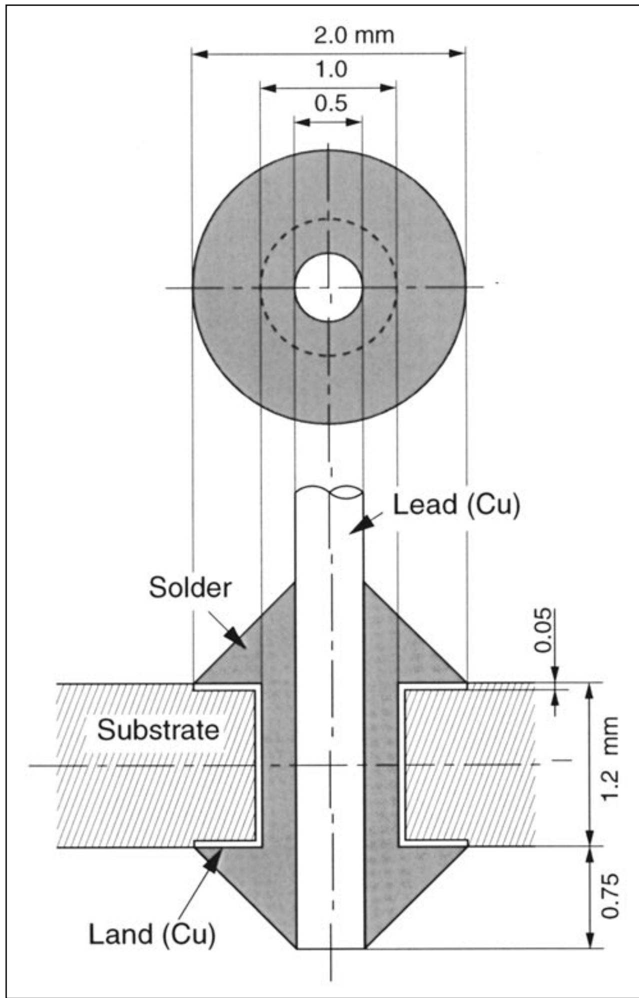

Fig. 12. Cross-sectional view of the axis of revolution of the simulated soldering components.

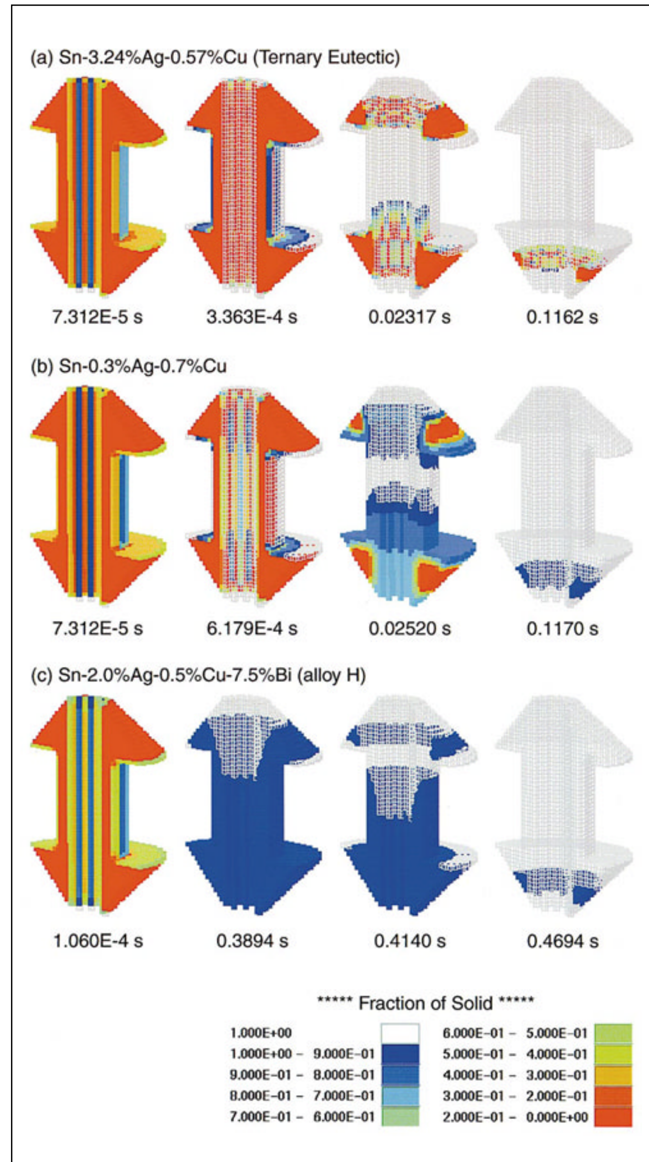

Fig. 13. Evolutions of solidification of (a) Sn-3.24%Ag-0.57%Cu, (b) Sn-0.3%Ag-0.7%Cu, and (c) Sn-2.0%Ag-0.5%Cu-7.5%Bi alloys.

solidification, which causes an extensive fall of terminating temperature of solidification as shown in Fig. 11a. The temperature, 139.9°C, corresponds to the eutectic reaction of the Sn-Bi binary system. The behavior of such a residual liquid phase at low temperatures is considered to cause lifting-off failure at the interface between the solder material and the Cu land.

Three-dimensional solidification simulation was performed on the soldered material that connects a Cu lead wire and a Cu land attached to a hole through the substrate. A cross-sectional view taken of the axis of revolution is shown in Fig. 12, and all the components are sectioned into 0.025 mm cubic elements. The conditions of the simulation are shown in Table II. Figure 13 shows the evolutions of solidifying soldering materials where the fractions of solid of each element are distinguished by their colors as shown in the legend of Fig. 13. Transparent elements with grids correspond to completely solidified material. In the case of the ternary eutectic alloy shown in Fig. 13a, solidification starts from the interface between the solder alloy and the Cu lead wire and proceeds with small heterogeneity of the solid fraction. Nevertheless, a small amount of the liquid phase remains in

Table II. Properties for Solidification Simulation

	Density [kg/m^3]	Specific Heat [J/kg · K]	Thermal Conductivity [W/m · K]	Latent Heat [J/kg]
Solder	7300	226	30	Figs. 10b and 11b
Cu (Lead & Land)	8930	386	385	—
Substrate	1800	799	0.3	—

most of the cubic elements and a mushy type of solidification takes place in alloy-H because of the wide range of solidifying temperature due to non-equilibrium solidification. In this simulation, transfers of alloying elements across the boundary of cubic cells are not taken into account. Thus, the macroscopic segregation cannot be simulated. Further development of the simulating model is necessary for explaining the mechanism of lifting-off failures.

CONCLUSION

Phase equilibria in the Sn-Ag-Cu ternary system were investigated and the thermodynamic assessment of the alloy system were completed based on the results of the determined phase boundaries as well as previous experimental data. The results were incorporated into the thermodynamic database of the micro-soldering alloys, making it possible to predict not only phase equilibria but also other properties such as surface tension, viscosity and the non-equilibrium solidification process. The three-dimensional solidification process was simulated by making use of the calculated properties by the CALPHAD method. There is still room for improvement in the simulation of the practical solidification process. The database of the micro-soldering alloys should prove to be quite useful for alloy design and the development of Pb-free solder alloys.

ACKNOWLEDGEMENT

The authors wish to thank the support from Casio Science Promotion.

REFERENCES

1. *Lead Free Solder Project, Final Report,* NCMS Report 0401 RE 96 (Ann Arbor, MI: National Center for Manufacturing Science, August 1997).
2. I. Ohnuma, X.J. Liu, H. Ohtani, and K. Ishida, *J. Electron. Mater.* 28, 1164 (1999).
3. I. Ohnuma, X.J. Liu, H. Ohtani, and K. Ishida, *Functional Materials,* ed. K. Grassie et al. (Weinheim, Germany: Wiley-VCH, 2000), p. 69.
4. N. Saunders and A.P. Miodownik, *CALPHAD* (Lausanne, Switzerland: Pergamon, 1998).
5. U.R. Kattner and W. Boettinger, *J. Electorn. Mater.* 23, 603 (1994).
6. F.H. Hayes, L. Lukas, G. Effenberg, and G. Petzow, *Z. Metallkd.* 77, 749 (1986).
7. J.-H. Shim, C.-S. Oh, B.-J. Lee, and D.-N. Lee, *Z. Metallkd.* 87, 3 (1996).
8. A. Dinsdale, *CALPHAD* 15, 317 (1991).
9. I. Karakaya and W.T. Thompson, *Bull. Alloy Phase Diagrams* 9, 144 (1988).
10. E.Y. Tonkov and I.L. Aptebar, *Dokl. Acad. Nauk. SSR* 188, 401 (1969).
11. H. Ohtani, K. Okuda, and K. Ishida, *J. Phase Equilibria* 16, 416 (1995).
12. H. Ohtani, M. Miyashita, and K. Ishida, *J. Jpn, Inst. Met.* 63, 685 (1999).
13. O. Bauer and O. Vollenbruck, *Z. Metallkd.* 15, 119 (1923).
14. M. Hamasumi and Y. Odamura, *J. Jpn, Inst. Met.* 1, 165 (1937).
15. X.-J. Liu, C.P. Wang, I. Ohnuma, R. Kainuma, and K. Ishida, to be submitted to *J. Alloys and Comp*.
16. B. Sundman, B. Jansson, and T.O. Anderson, *CALPHAD* 9, 153 (1985).
17. E. Gebhardt and G. Petzow, *Z. Metallkd.* 50, 597 (1959).
18. J.A.V. Butler, *Proc. Roy. Soc.* A135, 348 (1932).
19. T. Tanaka and I. Iida, *Steel Research* 65, 21 (1994).
20. S. Seetharaman and D. Sichen, *Metall. Mater. Trans. B* 25B, 589 (1994).
21. S. Hao, K. Anzai, and E. Niyama, *Trans. AFS* 103, 41 (1995).
22. J.H. Vincent, B.P. Richards, D.R. Wallis, I.A. Gunter, M. Warwick, H.A.H. Steen, P.G. Harris, M.A. Whitmore, S.R. Billington, A.C. Harman, and E. Knight, *Circuit World* 19, 32 (1993).